Energy-absorbing origami structure for crashworthiness design

Energy-Absorbing Origami Structure for Crashworthiness Design

Leonardo Marconi [a,b], Yong-Ha Hwang[a], Jae-Hung Han*[a], Giacomo Frulla[b], Enrico Cestino[b]
[a]Dept. of Aerospace Engineering, Korea Advanced Institute of Science and Technology, 291 Daehak-ro, Yuseong-gu, Daejeon, Republic of Korea; [b]Dept. of Mechanical and Aerospace Engineering, Politecnico di Torino, Corso Duca degli Abruzzi 24 -10129 Torino, Italy

ABSTRACT

This paper presents experimental and numerical investigations on the origami-patterned tube which is acknowledged as a promising energy-absorption device. Its buckling mode leads to high performances in terms of specific energy absorption (SEA) and crush force efficiency (CFE). The polygonal tube is prefolded by following an origami pattern, which is designed to act as geometric imperfection and mode inducer. First, a series of quasi-static crushing tests are performed on origami tubes with different materials and geometrical features. Specimens in SUS316L and AlSi10Mg are produced through Additive Manufacturing (AM). It allows to conveniently produce few samples with a complex shape. Finite Element Analysis (FEA) and Direct Image Correlation (DIC) are employed for a better insight into the complex crushing behaviour. The Aluminum tube shows a brittle behaviour while SUS316L tubes have extremely promising performance until local crack happens. Limits stemming from the employment of AM are explored and a new geometry is designed to avoid cracking. Second, a numerical design exploration study is carried out to assess the sensitivity of origami pattern features over the energy-absorption performance. ANSYS Autodyn is utilized as FE solver and DesignXplorer for correlation and optimization. The benefits of new patterns are investigated through geometrical optimization, and an improved geometry is proposed. The pattern stiffness is tuned to account for the external boundary conditions, resulting in a more uniform crushing behaviour. A similar force trend is maintained with a SEA increment of 51.7% due to a drastic weight reduction in areas with lower influence on post-buckling stiffness.

Keywords: Origami, Crashworthiness, CFE, SEA, Diamond buckling, Energy absorber, FEM, Additive Manufacturing

1. INTRODUCTION

The present investigation is the starting point and a feasibility study for a future application of the origami-patterned tube as a crashworthy component on a Personal Air Vehicle (PAV). A crashworthy design has become a main requirement for all manned vehicles. In particular, it has always remained a top priority to prevent casualties for helicopters[1]. The structure must be designed to lower accelerations on the occupants in the event of a crash, until a survivable level. An energy-absorbing device is fundamental for this purpose. Thin-walled tubes under axial crushing are commonly employed for this purpose[2]. However, they present significant drawbacks. First, their high buckling peak force is critical for crashworthy applications in which the maximum force is limited by the human body's tolerance. Second, straight tubes collapse in natural modes, inducing a naturally set wavelength that results in a limited energy absorption[3]. Flat force trend and lightweight are primary requirements for the crashworthy application on a flying vehicle, thus Specific Energy Absorption (SEA) and Crush Force Efficiency (CFE) are selected as performance parameters:

$$\mathrm{SEA}=\frac{\mathrm{E_{absorbed}}}{\mathrm{W_{structure}}}=\frac{\int_0^{\delta_{\mathrm{stroke}}}\mathrm{F_{(x)}}\,\mathrm{dx}}{\mathrm{W_{structure}}}\quad\left[\frac{\mathrm{kJ}}{\mathrm{kg}}\right] \tag{1}$$

$$\mathrm{CFE}=\frac{\mathrm{F_{mean}}}{\mathrm{F_{max}}} \tag{2}$$

where $\mathrm{E_{absorbed}}$ is the area under the force-displacement curve of the tube under compression, $\mathrm{W_{structure}}$ is the absorbing structure weight, F_{mean} is the averaged of reaction force through the crushing stroke and F_{max} is the peak reaction force.

*jaehunghan@kaist.ac.kr; phone +82-42-350-3723; http://sshs.kaist.ac.kr

Active and Passive Smart Structures and Integrated Systems XVI, edited by Jae-Hung Han
Shima Shahab, Jinkyu Yang, Proc. of SPIE Vol. 12043, 1204303
 · 0277-786X · doi: 10.1117/12.2614384

Various techniques have been developed to increase the energy absorption and to smooth the initial force peak. For the latter purpose, geometrical discontinuities such as holes, dents, or corrugations are often employed. However, SEA can be lower than their equivalent straight tube[4]. The origami-patterned crash box is a thin-walled energy-absorber designed to induce the high energy absorption "diamond" buckling mode. It also acts as an induced geometrical discontinuity, to flatten the crushing force trend. Recent investigations show the high potential of origami configurations. Numerical optimizations through FEM analysis exhibit CFE up to 90% and SEA up to 87% higher than the conventional square tube[5] or 49% higher than the hexagonal configuration[6]. High performances, lower weight due to higher SEA, and convenient manufacturability make this configuration a potential candidate for this aeronautic application.

2. EXPERIMENTS ON ADDITIVE MANUFACTURED SPECIMENS

2.1 Test Objectives

Direct Metal Laser Sintering (DMLS) is selected to produce the origami tubes. It guarantees the possibility of manufacturing small batches of complex specimens with advantages in terms of cost and time, compared to traditional approaches[7]. This investigation aims to assess the prospect of manufacturing energy-absorbing origami tubes through DMLS. The experimental outcomes are evaluated in terms of triggered collapsing mode, performances, and predictability of the behaviour through numerical analysis. The experiments are intended to provide a reference case, and thus the starting point, for the following geometrical optimization of the pattern for a future application in the PAV crashworthiness design.

2.2 Quasi-static test setup

The specimens are printed in SUS316L and AlSi10Mg using an EOS M290 machine. The build direction is coincident with the tube vertical axis. Their pattern is based on a previous study from Zhou C. H. et al. on a stamped mild steel geometry[8]. The nominal wall thickness is 1.5 mm due to the initial technological limit in the 3D printing method. The geometry in Figure 1 is characterized by 156° prefolding angle (θ), 60 mm edge length (b), 20 mm lobe length (c), 3 equal modules (M) and 117.38 mm of total height (h). Tubes are measured before testing and an excellent agreement with the CAD geometry is found, except for the wall-thickness measured to be 1.58 ±0.02 mm. Three origami-patterned tubes with identical geometry are initially printed and tested: one in AlSi10Mg and the other two in SUS316L.

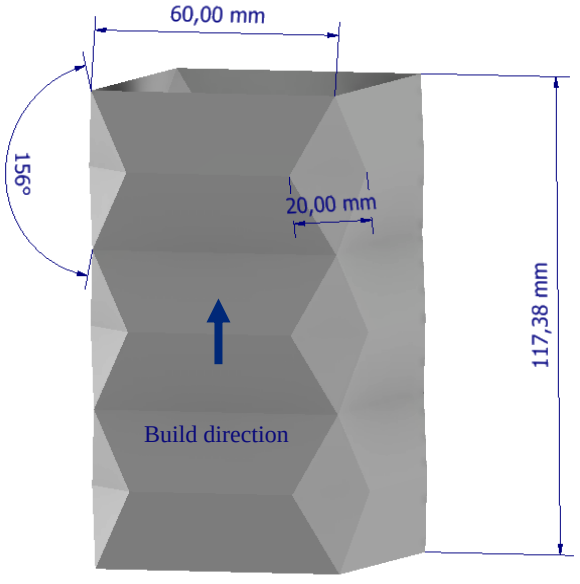

Figure 1 Printed origami-patterned tube surface geometry and build direction

The quasi-static tests are conducted using an Instron Universal Testing Machine (UTM). The tube stands on a thick plate while the crosshead connected to the load cell moves downward. Both ends of the tube are free of constraints. Digital Image Correlation (DIC) is employed to compute deformation and strain on the tube surface. The test is under displacement control, with a crosshead velocity of 0.6 mm/min. The strain rate is checked through DIC to ensure the quasi-static regime.

2.3 Quasi-static test results

The employment of AlSi10Mg can considerably reduce the structure weight, with potential benefits in SEA. However, the crushing of this specimen shows an extensive occurrence of fractures, which severely undermine the performance. The crack emerges at the interface between the tube edge and rigid plate, suddenly propagating along the edges of the pattern. The crushing is dominated by large crack propagation, resulting in a strain localization at the cracking region. The tube starts cracking at a reaction force of 20 kN during its initial elastic slope, and it suddenly drops until around 2 kN due to fractures, without triggering the expected diamond mode. The material fails in a completely brittle manner, therefore, AlSi10Mg is not suitable for realizing crashworthy origami structures which need to undergo large plastic deformation.

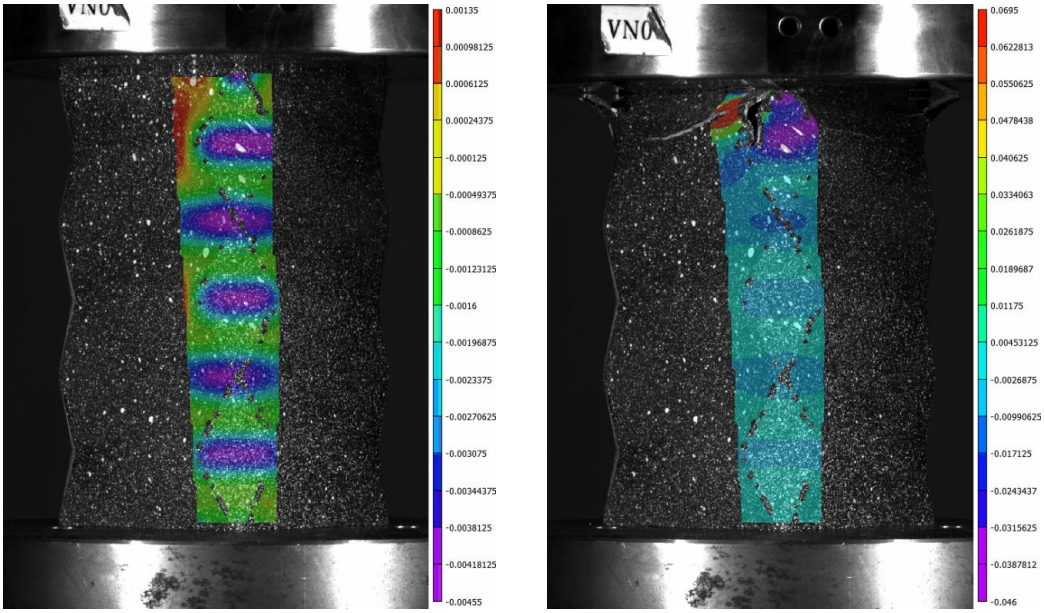

(a) (b)

Figure 2 DIC axial strain of the AlSi10Mg 1.58 mm thick specimen: (a) pre-fracture, (b) post-fracture

Additive manufactured SUS316L has excellent mechanical properties, which make it a good candidate for its use in energy-absorbing components. The stainless-steel origami exhibits exceptionally promising results in the first part of the test. The specimen successfully buckles and triggers the expected diamond mode, maintaining a nearly constant reaction force in its post-buckling stroke. It eventually suffers from localized cracking in the edges of the lobes under tensile stress. The fracture compromises the pattern stiffness of the module, heavily affecting the force output. The force peak in Figure 3 is due to the first module's bottoming out, which lets the adjacent module buckle and consequently crack in the same manner.

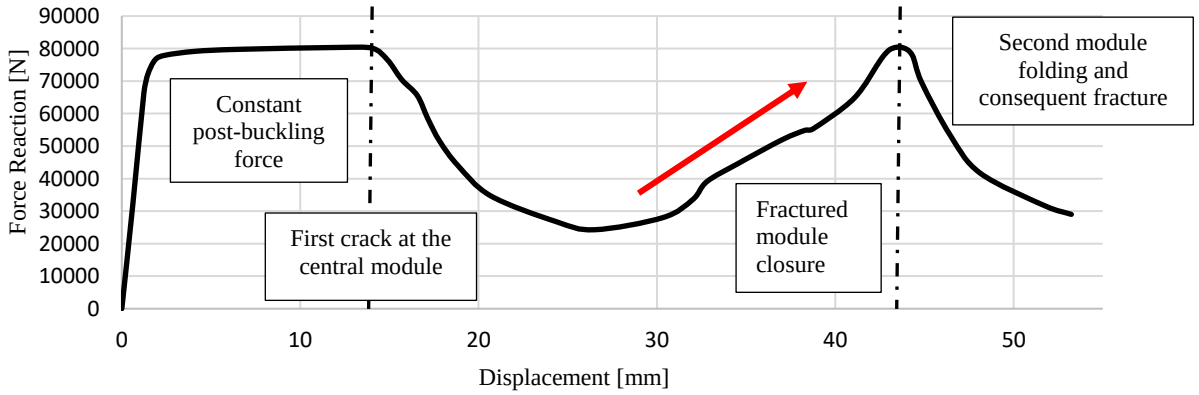

Figure 3 Force - Displacement curve of the SUS316L 1.58 mm thick specimen

A complex 3D strain field is noticeable at the corners under tension as shown on the right-hand side corner in Figure 4.

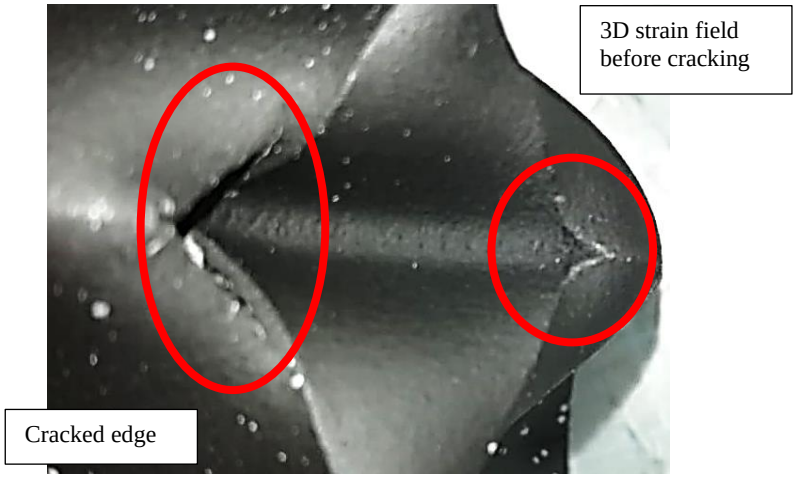

Figure 4 Partially crushed module of the SUS316L 1.58 mm thick specimen

A second identical SUS316L specimen is annealed to seek increased ductility as a first trial to avoid cracking. The annealing procedure is performed in three steps until a temperature of 1050°C in a vacuum atmosphere. Nevertheless, the annealed specimen exhibits a similar trend, with a constant force of 60 kN, and experiencing fractures at the same stroke.

2.4 Numerical study and quasi-static test on new geometry

The causes of the problem encountered in the SUS316L specimen are investigated through explicit FEM analysis. The solver Autodyn by ANSYS is employed. The numerical model replicates the experimental test conditions. The tube stands between two rigid panels modelled with rigid shell elements. The bottom plate has fixed displacement while the upper one has a downward axial velocity boundary condition for a total crushing stroke of 70 mm. The velocity is ramped at the beginning of the crushing to reduce the initial contact force oscillation. Since the tube is expected to buckle progressively[9], only a quarter of the tube is modelled in the simulation by assigning symmetry conditions at the two planes of symmetry. The assumption is validated against the full model. The body self-contact algorithm is employed, with a value of 0.3 for both static and dynamic friction coefficients. A fully quad mapped mesh is formed by reduced integration linear shell elements with 5 integration points through the thickness. A global mesh size of 2 mm and end time of 0.02 s are chosen in accordance with the mesh and timestep sensitivity analysis. A series of 10 tensile tests on specimens printed in parallel and normal direction to the load is given from the manufacturer. Properties are computed in mean value and standard deviation for both printing directions. An isotropic material model with averaged properties is employed for the analysis since the test indicates a minor orthotropy of the material.

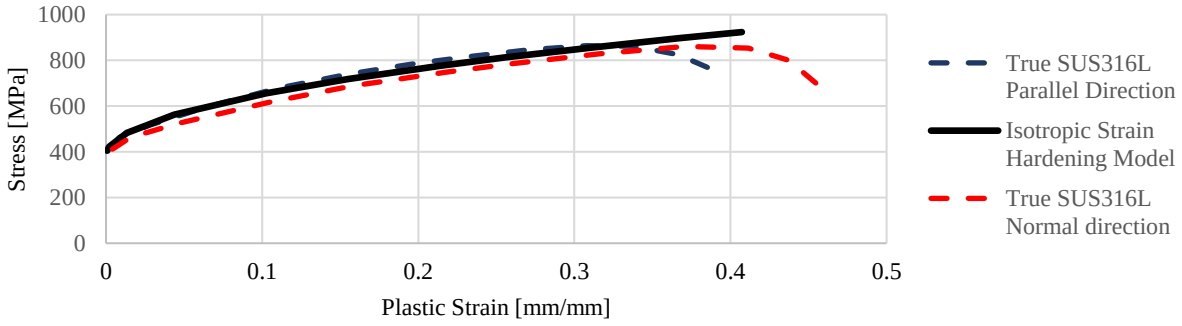

Figure 5 Representative engineering stress-strain curve of SUS316L printed in normal and parallel direction to the load

The mean mechanical properties are 204 GPa Young's modulus, 420.5 MPa yield stress and 0.53 max engineering strain. The Ludwik plasticity model employed is reported in Equation 3. The hardening coefficients n and K are computed through a first-order regression of the bi-logarithmic stress to plastic strain curve[10]. The resulting curve is shown in Figure 5.

$$\sigma = \sigma_{Yield} + K\varepsilon_{plastic}^{n} \tag{3}$$

The FE model underestimates the buckling force, while it has an upward force trend after buckling. The subsequent force drop is due to the cracking. The initial discrepancy between FEM and experiment could be attributed to 3D strain fields and material properties uncertainty. The shell element formulation used cannot model strain in thickness direction, which is visible in specific areas. Also, the provided material characterization is not representative of our specific printing job.

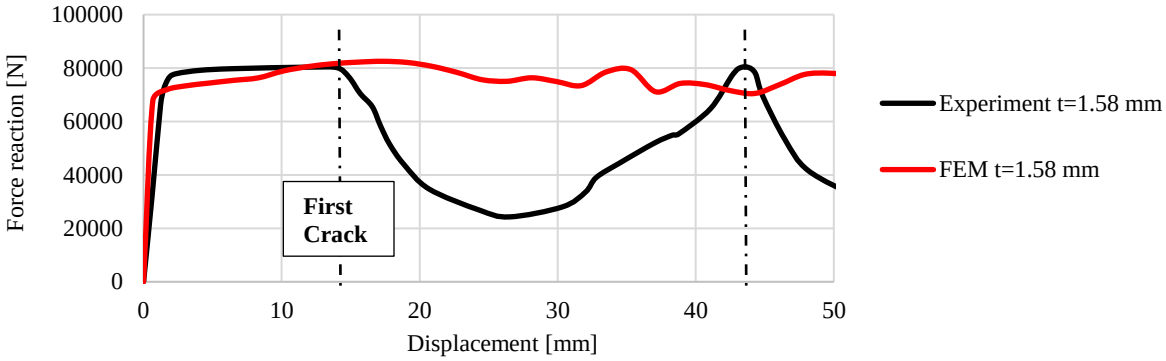

Figure 6 Comparison between experiment and FEM for the SUS316L 1.58 mm thick specimen

The problem was found in the stiff behaviour of the surfaces that compose geometry. They concentrate the stress on the plastic hinges (pattern creases) rather than deforming themselves. Two features are numerically investigated to solve the crack issue. First, increased compliance of the surfaces is sought by lowering the wall thickness to 1 mm. Weight decreases linearly with the thickness, while the absorbed energy is found to have a stronger decreasing trend. As a result, SEA decreases from 13.9 kJ/kg to 9.75 kJ/kg, for the 1.58 mm and 1 mm thick tubes respectively. Second, a rounded fillet with a 2 mm radius is applied to all pattern creases, to avoid stress concentrations at the sharp edges. This feature affects the performances to a minor extent. As shown in Figure 7, the modifications induce a large area around the plastic hinges to deform, expanding the lobe beyond its prefolded shape.

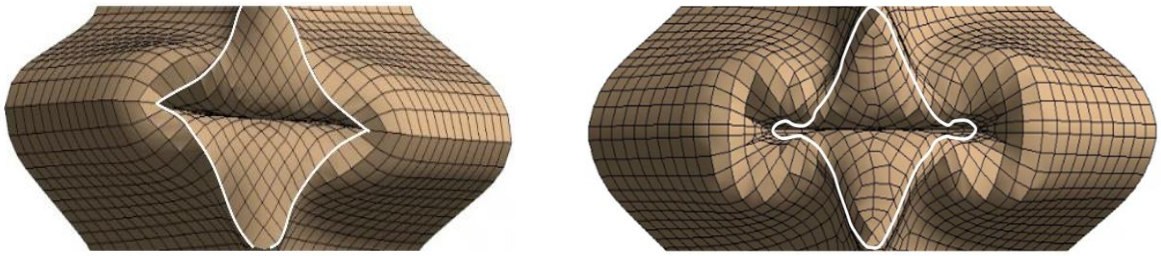

(a) (b)

Figure 7 Numerically crushed lobe: (a) sharp-edged 1.58 mm thick origami, (b) 2 mm fillet radius 1 mm thick origami

The new specimen is eventually printed in SUS316L and tested. In accord with the FE study, a smoother transition between the lobe surface and the adjacent surfaces is achieved. However, this specimen also suffers from fracture, but in one side of the lobe only. Consequently, the tube stiffness is to some extent preserved, and thus, the drop in reaction force is lower than in the previous case. Finally, the 3D strain field at the lobe edges is no more evident.

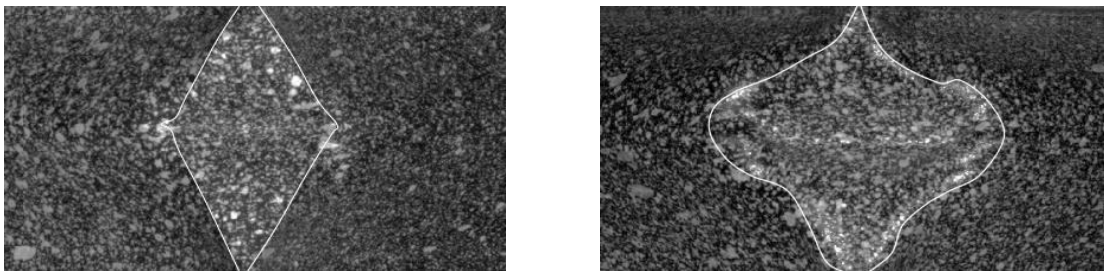

(a) (b)

Figure 8 Lobe geometry before cracking: (a) sharp-edged 1.58 mm thick origami, (b) 2 mm fillet radius 1 mm thick origami

3. DESIGN EXPLORATION AND OPTIMIZATION

3.1 Aim and methodology

A numerical design exploration study is performed to evaluate the influence of the pattern on crashworthiness performances. Four geometric inputs and two performance outputs (CFE, SEA) are chosen for this purpose. The boundary conditions are defined to be representative of a real application. Design of Experiments (DOEs) is employed to assess the sensitivity of performances to geometric parameters and individuate the ones with a major impact on the problem. Next, the optimization is carried out to investigate the potential benefits of a new pattern. The DesignXplorer tool by ANSYS is employed for the study. The FE model is validated against the experiments[8] from Zhou C. H. et al. The publication is used as the reference case since the mild steel origami tubes successfully collapse in diamond mode without fractures.

3.2 Parametric Geometry and FE model

The geometry is defined by 29 parameters dependent on 4 design parameters through the origami congruence equations. The parameters are: prefolding angle of the internal module (θ_{int}), edge length (b), lobe aspect ratio (c_2/c_1) and height ratio (h_{int}/h_{ext}). The number of modules is set to 3, the wall thickness to 1 mm and the tube height ($\mathrm{h_{tube}}$) to 120 mm.

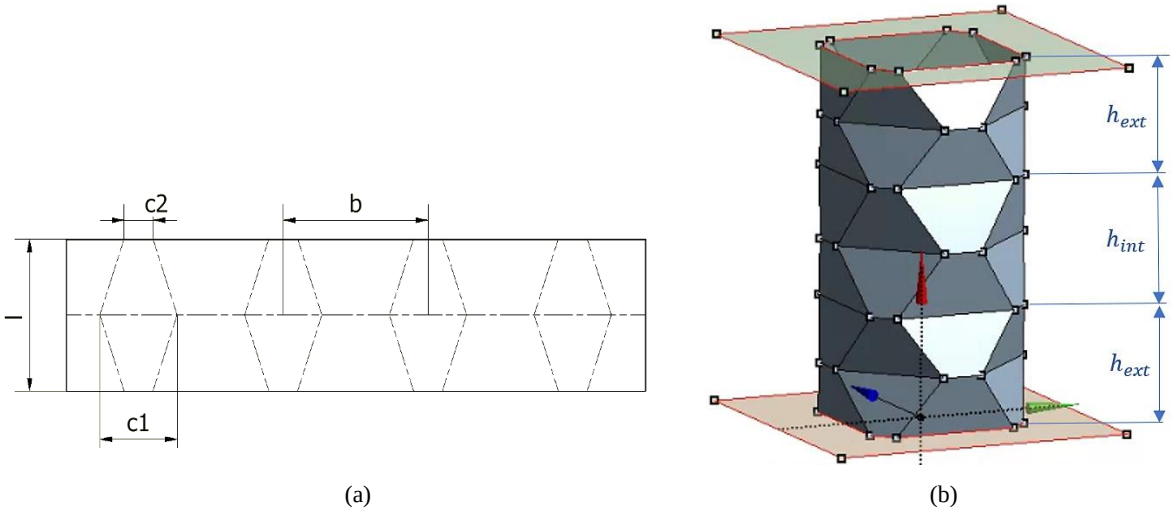

(a) (b)

Figure 9 Parametric geometry: (a) folding lines on flat sheet, (b) folded origami tube

Nodes at both tube ends are fixed in non-axial displacement, in order to preserve the cross-section. The constraint aims to model the scenario in which the origami is welded to a thin-walled plate, characterised by the low resistance to bending moments of joint and support. The novel parameter height ratio is introduced to tune internal and external modules stiffness, by acting on the external modules' prefolding. The basic reason is that external modules with one fixed cross-section have different stiffness compared with the internal module that shrinks at the interfaces with external modules.

The origami congruence equations[11] for prefolding angles are rewritten, for considering the height ratio:

$$\operatorname{cotg}\left(\frac{\theta_{\mathrm{int}}}{2}\right) = \frac{\left(\sqrt{2}-1\right) c_1 \left(1-\left(\frac{c_2}{c_1}\right)\right)\left(1+2\left(\frac{h_{\mathrm{ext}}}{h_{\mathrm{int}}}\right)\right)}{h_{\mathrm{tube}}} \tag{4}$$

$$\operatorname{cotg}\left(\frac{\theta_{\mathrm{ext}}}{2}\right) = \frac{\left(\sqrt{2}-1\right) c_1 \left(1-\left(\frac{c_2}{c_1}\right)\right)\left(2+\left(\frac{h_{\mathrm{int}}}{h_{\mathrm{ext}}}\right)\right)}{h_{\mathrm{tube}}} \tag{5}$$

Material data are given in the publication[8]. Dynamic effects are not considered and only a quarter of geometry is modelled. The Uniform MultiZone Quad/Tri meshing algorithm with a mesh size of 1.5 mm is used. The model validation is performed without the fixed cross-section constraint at the tube edges. A good agreement is found between the FE model and the two experiments available in the literature. All the cases are found comparable in force trend.

3.3 Parameter correlation and optimization

The automatic DoEs algorithm of DesignXplorer is used to sample the domain defined in Table 1. Geometric parameters are then correlated with the resulting performances. The conclusions drawn at this phase are used to guide and constrain the design space for the following optimization.

Table 1 Design exploration domain

Prefolding angle (ϑ_{int})	Edge length (b)	Lobe area ratio (c_2/c_1)	Height ratio (h_{int}/h_{ext})
150° to 170°	50 mm to 60 mm	5% to 25%	0.75 to 1.25

The tube mass is influenced nearly completely by the edge length, while the mean reaction force appears to have a lower sensitivity to the parameter. As a result, a small edge length advantages the SEA in the selected range of values. Due to its implementation, the edge length does not influence the lobe geometry, which is fully defined the other three parameters. A minor influence on the performances of interest is found for the lobe aspect ratio.

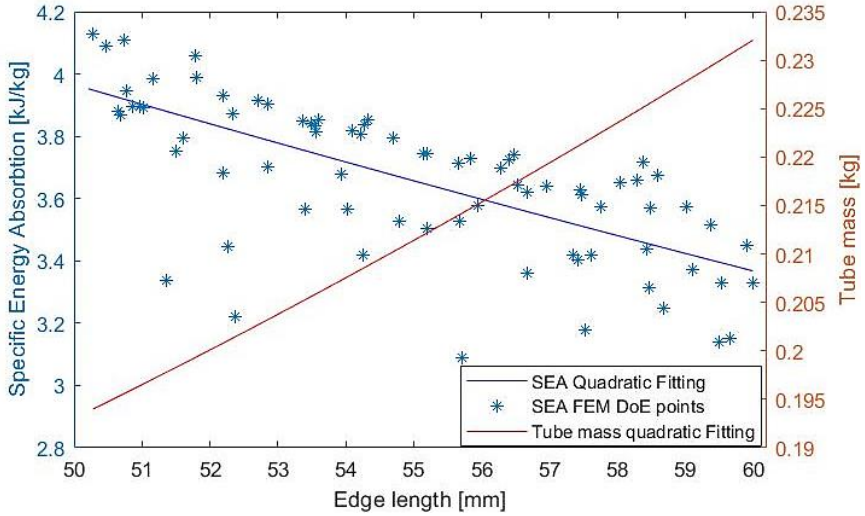

Figure 10 Edge length influence on tube weight and SEA

The optimization aims to maximise the specific energy absorption for a given set of geometrical constraints and within a maximum reaction force. According to the precedent design exploration two modifications are applied to the design space:

- $c_2 = 2.1\ mm$ The parameter lobe aspect ratio is removed, a constant 1.5x45° fillet is used instead
- $155° \leq \vartheta \leq 165°$ The domain is limited to avoid bottoming out and local or non-diamond buckling

Boundaries and geometric constraints of the optimization problem:

- F_{max} ≤13.75 kN Maximum force reaction lower than the original configuration
- $b - c_1 \geq 20\ mm$ To avoid adjacent lobes interaction and to leave space for welding
- $b \geq 40\ mm$ Limit on the minimum moment of inertia of the narrowest section

Response surfaces are computed, and an optimized configuration is individuated and simulated through FEA.

Table 2. Optimized origami-patterned tube geometry

Prefolding angle (ϑ_{int})	Edge length (b)	Height ratio (h_{int}/h_{ext})
162°	40 mm	1.11

The smaller cross-section drastically reduces to tube mass, while its post-buckling stiffness is compensated by a stiffer pattern geometry. An increase of 51.7% in SEA is obtained with the optimised origami pattern. Finally, the tuned axial stiffness permits also to the external side of the external module to deform correctly, as shown in Figure 11.

Table 3 Performance comparison between optimized and reference origami-patterned tubes

	$Mass$ [g]	F_{max} [kN]	F_{mean}[kN]	CFE[%]	SEA [kJ/kg]
Reference	232.3 g	13.76	10.97	79.8 %	3.271
Optimized	153.6 g	13.01	11.01	84.7 %	4.963
Difference [%]	↓↓ 34 %	↓ 5.4 %	≈	↑ 4.9 %	↑↑ 51.7 %

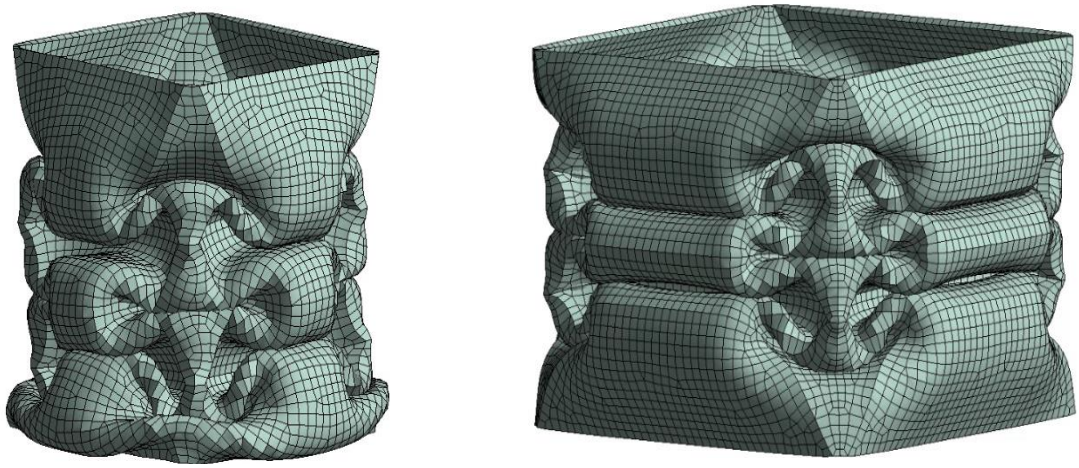

(a) (b)

Figure 11 Crushed origami tubes (70 mm stroke): (a) optimized, (b) reference geometry

4. CONCLUSIONS

Crashworthiness characteristics of the origami-patterned tube are explored in this paper through experiments and numerical simulations. At first, a series of quasi-static crushing tests are performed on origami tubes produced through Additive Manufacturing. Two materials are chosen: AlSi10Mg and SUS316L. The aluminium sample reveals a brittle behaviour which results in poor energy absorption due to a collapsing mode dominated by cracks propagation. The stainless-steel origami exhibits excellent performances before suffering from localised fractures at the lobe corners under tension. The problem is individuated in the stiff behaviour of the pattern surfaces, which tend to concentrate stress at the plastic hinges instead of bending themselves. A new geometry is numerically studied to solve the issue by enlarging the area undergoing deformation around the point that triggers the fracture. The new tube characterised by rounded fillets and lower thickness is finally printed and tested. The sample also cracks although to a lesser extent, partially preserving its post-buckling stiffness. The few available materials for metal 3D printing and the technological constraint set on the minimum thickness of 1 mm, represent a severe limitation to producing energy-absorbing origami tubes. Furthermore, material properties are highly dependent on the printing process, introducing inevitable uncertainties in the FEM model. Secondly, the potential benefits of a new origami pattern are investigated through geometrical optimization, and consequently, an improved geometry is proposed. A previous publication is adopted to validate the FE model. Boundary conditions and design constraints are set to be representative of a real application scenario. The parametric study suggests that the tube axial stiffness in the post-buckling regime is mainly driven by the lobe geometry. Prefolding angle and its distribution due to the height ratio are found to be influential on the resulting reaction force. Edge length has also a major influence on the force output, and at the same time, it is strictly correlated with the tube weight. An increment of 51.7% in SEA is achieved for the optimised origami geometry due to a drastic weight reduction outside the lobes' area and a stiffer pattern.

ACKNOWLEDGEMENTS

This research work is carried out at the Smart Structures and H/W Systems Laboratory (Korea Advanced Institute of Science & Technology) as part of the "thesis abroad" programme of Politecnico di Torino.

REFERENCES

[1] Yang, X., Ma, J., Wen, D., and Yang, J., "Crashworthy design and energy absorption mechanisms for helicopter structures: A systematic literature review", Progress in Aerospace Sciences, 114 (2020).
[2] Alghamdi, A. A. A., "Collapsible impact energy absorbers: an overview," Thin-walled structures, 39(2), 189-213 (2001).
[3] Song, J., Chen, Y., and Lu, G., "Axial crushing of thin-walled structures with origami patterns," Thin-Walled Structures, 54, 65-71 (2012).
[4] Singace, A. A., and El-Sobky, H., "Behaviour of axially crushed corrugated tubes," International Journal of Mechanical Sciences, 39(3), 249-268 (1997).
[5] Zhou, C., Zhou, Y., and Wang, B., "Crashworthiness design for trapezoid origami crash boxes," Thin-Walled Structures, 117, 257-267 (2017).
[6] Ma, J., Dai, H., Shi, M., Yuan, L., Chen, Y., and You, Z., "Quasi-static axial crushing of hexagonal origami crash boxes as energy absorption devices," Mechanical Sciences, 10(1), 133-143 (2019).
[7] Spierings, A. B., Levy, G., Labhart, L., and Wegener, K., "Production of functional parts using SLM–Opportunities and limitations," 5th International Conference on Advanced Research in Virtual and Rapid Prototyping, 785-790 (2011).
[8] Zhou, C. H., Wang, B., Luo, H. Z., Chen, Y. W., Zeng, Q. H., & Zhu, S. Y., "Quasi-static axial compression of origami crash boxes," International Journal of Applied Mechanics, 9(05), (2017).
[9] Abramowicz, W., and Jones, N., "Transition from initial global bending to progressive buckling of tubes loaded statically and dynamically," International Journal of Impact Engineering, 19(5-6), 415-437 (1997).
[10] Murugesan, M., and Jung, D. W., "Johnson Cook material and failure model parameters estimation of AISI-1045 medium carbon steel for metal forming applications," Materials, 12(4), 609 (2019).
[11] Ma, J., "Thin-walled tubes with pre-folded origami patterns as energy absorption devices," PhD Thesis, University of Oxford, (2011).